Title: Developmental co-emergence of cardiac and gut tissues modeled by human iPSC-derived organoids

Authors: A.C. Silva[1], O.B. Matthys[1,2], D.A. Joy[1,2], M.A. Kauss[1,3], V. Natarajan[1], M.H. Lai[1], D. Turaga[1], M. Alexanian[1], B.G. Bruneau[1,4,5,6], T.C. McDevitt[1,7,*]

Affiliations:

[1]Gladstone Institutes, San Francisco, CA.

[2]UC Berkeley-UC San Francisco Graduate Program in Bioengineering, San Francisco, CA.

[3]UC San Francisco Graduate Program in Biomedical Sciences, San Francisco, CA.

[4]Roddenberry Center for Stem Cell Biology and Medicine at Gladstone, San Francisco, CA.

[5]Cardiovascular Research Institute, University of California, San Francisco, CA.

[6]Department of Pediatrics, University of California, San Francisco, CA.

[7]Department of Bioengineering and Therapeutic Sciences, University of California, San Francisco, CA.

* Correspondence to: todd.mcdevitt@gladstone.ucsf.edu

Abstract:

During embryogenesis, organs in close proximity exhibit paracrine signaling that contributes to the development and fate of each tissue. Organoids are *in vitro* models that mimic tissue formation and heterogeneity, but lack the paracrine input of surrounding organs. Here, we describe a human multilineage iPSC-derived organoid that recapitulates cooperative cardiac and gut development, and exhibits greater morphological complexity than any single-lineage organoids described so far. In contrast with previous cardiac models devoid of endoderm (gut/intestine tissue), this organoid exhibited a heart wall-like structure, cardiomyocyte compartmentalization, enrichment of atrial/nodal cells, and functional maturation. Overall, this study demonstrates the ability to generate distinct functional tissues originating from different germ lineages within a single organoid model, an advance that will further the examination of multi-tissue interactions during development and disease.

One Sentence Summary:

Cooperative emergence of heart and intestine in an organoid recapitulates development and improves tissue-specific maturation.

Main Text:

Organoids provide an experimentally tractable approach to model tissue development and physiology *in vitro*. Specifically, organoids are *in vitro* models derived from stem cells or tissue progenitors that differentiate into multiple cell types in a spatially-organized manner, and whose function is similar to the tissue *in vivo* (*1, 2*). However, organoids typically represent an artificial scenario in which single tissues arise independently *in vitro*. Embryogenesis is a coordinated sequence of morphogenic events that regulates asymmetric co-emergence and self-organization of distinct cell populations in order to instruct organ formation (*3*). Physically juxtaposed organs/tissues that arise in close proximity to one another often exhibit paracrine signaling mechanisms that synergistically contribute to the developmental trajectory and eventual function of each tissue (*4, 5*). The heart is a prominent example in which proper formation requires precisely timed coordination between distinct cell populations, namely the first and second heart fields (FHF and SHF), neural crest cells, and the proepicardial organ, as well as paracrine signaling from adjacent developing tissues (*6, 7*). Therefore, due to the multifactorial complexity of cardiac development, it has been difficult to achieve an organoid model that recapitulates the structural and functional features of the heart. We hypothesized that creating an organoid with a permissive milieu for inducing the parallel emergence of cardiac and non-cardiac endoderm-derived tissue could support the development of a more complex *in vitro* model of the primitive heart. We generated 3D spheroids of early committed mesendoderm progenitors in a culture medium permissive of multi-lineage differentiation, which enabled the emergence of both mesoderm and endoderm cell lineages, resulting in multilineage organoids with formation of complex structures mimicking features of the developing heart and small intestine. Our model shows that the adjacent presence of endoderm tissue, in the form of intestine, contributes to the phenotypic and functional maturation of cardiomyocytes, as well as to their subtype-specification - characteristics not observed in conventional, endoderm-free cardiac microtissues or resulting from other differentiation methods. We therefore propose that multilineage organoids can serve as a new model system to provide essential insights into the crosstalk between tissues that occurs during embryogenesis, maturation and disease - a phenomenon that is difficult to dissect *in vivo*.

Formation of heart-like compartments in multilineage spheroids

We began by generating spheroids from mesendoderm progenitors differentiated for 5 days with the GiWi protocol (*8*). Spheroids were then cultured in conventional, cardiac-permissive medium supplemented with insulin (RPMI/B27+), or in an ascorbic acid (AA)-supplemented medium formulated for epicardial cell differentiation to mimic the signaling that occurs during cardiac differentiation and support the emergence of a variety of cell types (i.e. fibroblasts and smooth muscle cells (SMC) (*9, 10*) **(Fig. 1A,B)**. Noticeable differences between spheroids grown in conventional versus AA medium (hereafter referred to as “conventional” and “multilineage” microtissues, respectively) became evident within 2 weeks of differentiation. After 10 days, conventional microtissues displayed a spherical, uniformly translucent morphology with spontaneous contractility throughout **(Fig. 1C,E; Movie S1)**, whereas the multilineage microtissues exhibited a dark core of vigorously contracting cells surrounded by translucent non-contracting cells. Calcium transients were limited to the central region of contracting cells in the multilineage tissues **(Fig. 1C,D; Movie S2)**. Light sheet fluorescence microscopy of immunostained microtissues revealed that conventional microtissues were largely composed of cardiomyocytes, as identified by cardiac troponin (cTnT) immunostaining, that also co-expressed TBX18 **(Fig. 1E)**. In contrast, multilineage microtissues displayed a core of cTnT+

cardiomyocytes surrounded by a non-myocyte, stromal-like cell population (phalloidin+, cTnT-), and an outer layer of TBX18+ epicardial cells, a structure that closely resembles the radial organization of the embryonic heart wall **(Fig. 1E; S1A)**. Furthermore, after 30 days, multilineage microtissues were three-times larger in size (as measured by cross-sectional area) than the conventional microtissues, whose size remained largely unchanged **(Fig. 1F)**. During this period of dramatic growth, multilineage microtissues also exhibited a parallel increase in the volume of the cardiac region **(Fig. 1F, S2D; Movie S3-4)**. Cardiac growth appeared to result from cardiomyocyte proliferation based upon immunostaining for Ki67, a marker of active cell cycle—analogous to cardiac wall thickening during development **(Fig. S1C, S2D)**. Since the multilineage microtissues exhibited greater cellular and structural complexity than conventional microtissues, as well as comparable growth properties of the embryonic heart, we hereafter refer to them as multilineage organoids (*11*).

Long-term culture of multilineage organoids recapitulates embryonic heart and gut development

We next examined whether multilineage organoids acquired further complexity with extended time in culture. The growth trajectory of multilineage organoids accelerated throughout culture duration, with the average organoid reaching ~2mm in diameter after 100 days **(Fig. 2A-C)**. After 30 days, we identified the emergence of small epithelial cystic structures within the previously translucent layers of cells enclosing the cardiac core. These cystic structures expressed mid-hindgut (MHG) endoderm markers *FOXA2* and CDX2, therefore resembling primitive gut-like structures **(Fig. 2D; S2B,C)**. Within the cardiac regions of the organoids, a few ventricular cardiomyocytes (MLC2v+) appeared at the center of the cardiac tissue core (slow/fast TnI+) **(Fig. 2E)**, reminiscent of the spatial compartmentalization of atrial and ventricular cardiomyocytes in the primitive heart. After 50 days, the stromal cells surrounding the cardiac core were replaced by a mesenchymal tissue **(Fig. 2D)**, enriched in extracellular matrix (ECM) components, such as hyaluronic acid **(Fig. S2D)** and a fine fibrillar network of glycosaminoglycans **(Fig. 2D, light green/blue)**, that was populated by a few WT1-expressing cells **(Fig. S1A)**. The mesenchymal tissue resembled the interstitial tissue underlying the epicardium (or sub-epicardium) and the peritoneum (protective layer of the intestine) **(Fig. 2D)**. In addition, smooth muscle actin (SMA)-positive cells were detected at the surface of the organoid and in the sub-epicardium, while a few endothelial cells (Pecam-1+) appeared interspersed among the cardiomyocytes **(Fig. 2F)**. By day 60, SMCs (αSMA+ MYH7-) emerged prominently between the cardiac and the primitive gut-like tissue. The SMC tissue that arose between cardiac and gut tissue displayed slow and infrequent calcium transients (~5s duration per transient; 1-3 transients/minute) that corresponded with large contractions (>100 μm) which resembled peristalsis **(Fig. 2G,H; Movie S5-6)**. More endothelial cells were detected between the cardiomyocytes, forming branched-like structures resembling pre-vascular networks **(Fig. 2F)**. Between 70 and 100 days of differentiation, the primitive gut tissues matured, based upon the development of paneth cells (antimicrobial peptide-producing cells) and goblet cells (which produce mucins) **(Fig. 2D)**. Thus, multilineage organoids undergo a sequence of morphogenic events that recapitulates human embryonic cardiac and gut development, including the initial emergence of cardiac tissue followed by gut separated by interstitial tissue (sub-epicardium/sub-peritoneum-like tissue).

To assess the cellular heterogeneity of the multilineage organoids, we performed single-cell RNA-sequencing (scRNA-seq) on dissociated organoids after 100 days. scRNA-seq analysis

revealed 6 primary clusters consisting of enteric SMCs, fibroblasts, cardiomyocytes, gut, proliferating cells, and neuroendocrine cells **(Fig. 3A-C; S3A)**. The presence of neuroendocrine cells **(**expressing CHGA**; Fig. 3C; S3A)** suggests the development of chemosensing properties in the gut compartment (*12*). Additional subset analysis of the gut cluster confirmed the differentiation of specialized intestinal cells, including: 1) enterocyte-like cells (absorptive cells; expressing VIL1, ANPEP, MUC13/17); 2) paneth cells (expressing LYZ); 3) LGR5-expressing intestinal stem cells; and 4) small intestine cells marked by high expression of APOB, CDX2 and VIL1, along with enrichment of genes for glucose (SLC2A2) and cholesterol transporters (NPC1L1), and digestion (FABP2, SI, SLC5A1) **(Fig.3D,E; S3A,B)**. The presence of these gut cell types was further validated by electron microscopy of 100 day old multilineage organoids **(Fig. 2I i-v)**. Analysis of sub-populations within the cluster enriched for proliferative markers revealed the presence of proliferating cardiomyocytes (TTN, MYH6, NPPA) and SMCs (ACTG2, MYH11) **(Fig. S3C,D)**. Ki67 immunostaining demonstrated a decline over time in the number of actively cycling cells throughout culture **(Fig. 2J)**; nevertheless, some cardiomyocytes (slow/fast TnI+), SMCs, and gut cells were Ki67+ after 100 days in culture, corroborating the scRNA-seq results **(Fig. S3G)**. A sub-clustering analysis of the cardiomyocyte cluster indicated that after 100 days in culture, cardiomyocytes consisted of a mix of immature cells that co-expressed ECM genes and MYH11 **(Fig. 3F clusters 0 and 2; Fig. S3E)**, and mature atrial-like cardiomyocytes **(Fig. 3F,G cluster 1)** that expressed higher levels of TNNI3, MYH6 and NPPA **(Fig. 3G; S3A,E,F)**. A minority of cardiomyocytes (~30%) expressed IRX4 and MYH7, ventricular cardiomyocyte markers **(Fig. S3F)**, indicating that multilineage organoids favor the differentiation and maturation of atrial cardiomyocytes.

Multilineage organoids remained viable for over 1 year in culture, and stably maintained their millimeter size-scale and structural complexity **(Fig. S4)**. Contractile behavior was observed only when electrical stimulation was applied, a feature consistent with functionally mature iPSC-derived cardiomyocytes (*13*) **(Fig. S4B)**. The cardiac and intestine tissues remained polarized against opposite sides of the organoids, separated by stromal cells and SMCs **(Fig. S4C-E,G)**. In contrast to previous timepoints, small clusters of SMCs were detected amongst the cardiomyocytes, and were more pronounced at the boundary of cardiac tissue regions **(Fig. S4F)**. In addition, proliferating non-myocytes (Ki67+, cTnT-) were detected within the cardiac tissue, as well as mature looking blood vessel-like structures (lectin+ - a glycoprotein of the basal lamina of endothelial cells) embedded within or adjacent to the cardiac regions in some organoids **(Fig. S4C, G)**. Organoids cultured for 1 year proved challenging to dissociate to single cells, potentially due to the structural complexity and ECM composition of the organoids, thus limiting our ability to assay the cellular diversity of single cell transcriptomes or morphological features of individual cardiomyocytes.

Overall, these observations demonstrate that multilineage organoids represent a new type of compartmentalized organoid model that: 1) exhibits the co-development and maturation of tissues derived from two distinct germ layers (mesoderm and endoderm), and 2) allows the cardiac compartment to attain greater cellular and structural complexity than conventional iPSC-derived cardiac microtissues or engineered cardiac tissues (*14, 15*).

Multilineage organoids promote atrial/nodal cardiomyocytes specification and maturation

To further assess the maturity and sub-type specification of the cardiomyocytes, we performed electrophysiological and structural studies of the intact spheroids and dissociated cells. Over the course of time, 100% of conventional microtissues exhibited spontaneous

contractility and only 33±21% of day 80 conventional microtissues could be paced at 2Hz **(Fig. 4A; S5A,B)**. Furthermore, conventional microtissues revealed no dramatic changes over time in kinetic calcium handling properties (amplitude and stroke velocities) under 1Hz of stimulation, reflecting relatively immature function **(Fig. 4B,C)**. In contrast, multilineage organoids demonstrated a decrease in spontaneous calcium activity, from 100% at day 10 to 37±16% at day 100, and an ability to respond to higher frequencies of electrical stimulation, even up to 8Hz after 80 days of culture **(Fig. 4A-D; S5A)**. In addition, multilineage organoids demonstrated progressively increasing amplitude and maximum stroke velocities under 1Hz of stimulation after 30 days, consistent with greater functional maturation, in contrast to the conventional microtissues **(Fig. 4B,C).**

Morphological analysis of dissociated tissues revealed greater structural maturation of individual cardiomyocytes from day 30 multilineage organoids than conventional microtissues, as determined by greater surface area and perimeter, elongated morphology, and highly-aligned and defined sarcomeres **(Fig. 4E-G)** (*16*). More elongated cardiomyocytes with highly-aligned and defined sarcomeres were isolated from day 80 multilineage organoids, reflecting additional structural maturation over time **(Fig. 4F,G)**. Electron microscopic imaging of cardiomyocytes from day 100 multilineage organoids revealed a series of ultrastructural features typical of the third-trimester human fetal heart, including: 1) myofibrils closely packed with defined striations and no apparent M bands **(Fig. 4H,i)**; 2) cylindrical-shaped mitochondria aligned between the myofibrils **(Fig. 4H,ii)**; and 3) large pools of glycogen vesicles, the major energy source during fetal heart development **(Fig. 4H,iii)** (*17, 18*). This advanced degree of iPSC-derived cardiomyocyte structural features is not commonly observed, thus highlighting the ability of this organoid model to promote cellular maturation of cardiac muscle cells.

Patch-clamp analysis of dissociated single cardiomyocytes at day 30 indicated that multilineage organoids had a higher proportion of atrial/nodal-like cardiomyocytes (73%) than ventricular-like cardiomyocytes (27%), and the relative proportions remained unchanged at day 60 (80% atrial/nodal and 20% ventricular cardiomyocytes) **(Fig. 4 I,J)**. In contrast, conventional microtissues at day 30 contained a lower proportion of atrial/nodal-like cardiomyocytes (57%) **(Fig. 4I,J)**. These results reflect the unique ability of multilineage organoids to specify and mature atrial/nodal cardiomyocytes, which has been challenging to achieve by alternative differentiation methods (*15*).

The primary differences between the multilineage and conventional media were the concentrations of ascorbic acid (AA) and calcium. Previous studies have demonstrated that these two components can influence cardiomyocyte differentiation and maturation, respectively (*19, 20*). To assess the potential impact of different culture medium components alone on cardiomyocyte specification and maturation, patch-clamp analyses were performed in iPSC-cardiomyocytes differentiated in monolayer in conventional cardiac media (Ca^{2+}= 0.42mM), multilineage media (AA=100µg/ml, Ca^{2+}=1.05mM) and conventional cardiac media supplemented with AA and calcium (AA=100µg/ml, Ca^{2+}=0.63mM). The AA- and Ca^{2+}-supplemented conventional cardiac media enhanced cardiomyocyte maturation by promoting an increase in peak, amplitude and upstroke velocity (V/s) of the action potentials, but did not promote the emergence of atrial/nodal cardiomyocyte subtypes **(Fig. S5C-E)**. Consistent with these observations, cardiomyocytes differentiated in multilineage medium (in 2D monolayers) exhibited comparable maturation to those in the supplemented conventional media, but yielded mainly ventricular -like cells (97%) **(Fig. S5C-E)**. These data indicate that although the media components promoted functional maturation properties, they were not sufficient to direct

atrial/nodal specification. Furthermore, it suggests that the co-development of the small intestine, which is absent in conventional cardiac microtissues and 2D monolayers, appears to be a critical factor responsible for enrichment of atrial/nodal cardiomyocytes (73-80%; **Fig. S5D**) and maturation in multilineage organoids.

Multilineage organoids express cardiac and gut master regulatory genes

Many iPSC differentiation protocols are plagued by inherent variability in consistency (*2, 21*). In our system, when multilineage organoids failed to develop, spheroids instead yielded either solely cardiac microtissues or gut organoids **(Fig. 5A,B; S6)**. Despite batch-to-batch differences in spheroid phenotype, all spheroids (n>200) within a single batch derived from the same initial differentiation of progenitor cells manifested identical morphologies and cellularity **(Fig. 5A)**. Thus, we hypothesized that subtle differences in the cellular composition of the initial 2D cultures of differentiating cells were responsible for the phenotypic fate of the spheroids.

To evaluate the variability between the starting progenitor populations that gave rise to cardiac microtissues, multilineage organoids, or gut organoids, we performed a retrospective analysis of the initial progenitor cell population at day 5 of differentiation by bulk RNA-sequencing, immediately prior to spheroid formation **(Fig. 5B)**. Multidimensional scaling (MDS) analysis of the progenitor transcriptomes revealed that the different progenitors had distinct gene expression profiles, and that multilineage organoid progenitor cells represented a unique transcriptional state, roughly equidistant from both cardiac and gut progenitors **(Fig. 5C)**. A comparative analysis between cardiac microtissue and gut organoid progenitors demonstrated that cardiac microtissue progenitors displayed a muscle development-restricted gene expression program. In contrast, gut organoids revealed activation of a broader embryonic developmental program, including forebrain, heart, visual and sensory system development **(Fig. S7B)**. To dissect the specific transcriptomic features enabling multilineage organoid formation, differential expression analysis was performed to compare the multilineage transcriptional profile to gut organoid and cardiac microtissue organoid progenitors independently. Compared to cardiac microtissue progenitors, multilineage progenitors were enriched in genes related to muscle tissue development and function (*MYH6*, *MYOM1*, *TTN*), as well as transcription factors (TFs) expressed by cardiomyocytes (*MEF2C*, *NKX2-5*, *ISL1*) **(Fig. 5D)**, suggesting an increased cardiac signature in the multilineage progenitors. Compared to gut organoid progenitors, multilineage progenitors exhibited a gene expression enrichment of the muscle tissue development program (*ACTC1*, *MYH6*, *MYOM1*) **(Fig. 5E)**. No gene ontology term enrichment was observed for the gut organoid progenitors relative to the multilineage progenitors, presumably due to the fact that: 1) the population of gut progenitors express markers of early cardiac differentiation similar to the multilineage progenitors, 2) early time points (before 20 days) phenotypically resemble multilineage spheroids, 3) and gut tissue development required at least 2 months of 3D culture to manifest clearly **(with developed villi, Fig. 5A, S6, S7A; Movie S8)**. Histological analysis revealed that primitive gut structures emerged earlier in the gut organoids **(Fig. S7A, day 12)**, however similar structures were not seen in multilineage organoids until later time points **(Fig. 5A, day 20-30; Movie S8)**. Thus, the accelerated development of primitive cystic structures in gut organoids might have disrupted the cardiac morphogenesis present in multilineage organoids.

In order to dissect specific gene expression differences between multilineage and cardiac or gut progenitors, a targeted pairwise analysis was performed for relevant heart progenitors and endoderm-related genes. Most notably, multilineage progenitor populations expressed several

TFs expressed by cardiac cells (*ISL1*, *NKX2-5*, *TBX5*) and epicardial-related genes (*TBX18*, *SEMA3D*) at higher levels than cardiac progenitors **(Fig. 5F, top)**, consistent with the greater cardiac cell diversity observed in the multilineage organoids as compared to the cardiac microtissues **(Fig. 5A)**. Populations yielding multilineage organoids also expressed genes involved in gut tube development (*SOX17*, *ONECUT2*), although at lower levels than pure gut organoid progenitors, suggesting that the multilineage populations contained a smaller number or proportion of gut progenitors, based upon the initial endoderm transcriptional signature **(Fig. 5F,bottom)**. In total, multilineage organoid progenitors displayed a mixed transcriptomic profile of cardiac and gut progenitors, which could account for the observed co-emergence of heart and gut tissue together.

Distinct endoderm subtypes are known to play a role in cardiomyocyte formation through paracrine signaling mechanisms (*22, 23*). To examine potential intercellular paracrine signaling affecting the co-emergent populations, we compared the expression of genes associated with secreted factors between the different progenitor populations **(Fig. 5G)**. We first generated a list of secreted factors that were differentially enriched in the cardiac or gut progenitors **(Fig. S7D)**. FGF10 and NPPB were identified among the gut-enriched factors. FGF10 is a growth factor that enhances cardiogenic specification, fetal cardiomyocyte proliferation, and has been identified as an SHF-specific marker, indicating a role in heart tissue development (*24-27*). NPPB is highly expressed during cardiogenesis, particularly in the differentiating chamber myocardium (*28*). However, FGF10 and NPPB also promote intestinal cell proliferation, induction of goblet cell differentiation and homeostasis of mesenteric and intestinal tissue (*24, 25, 27, 28*). Thus, FGF10 and NPPB enhance aspects of both cardiac and gut tissue formation. Accordingly, multilineage progenitors expressed higher levels of FGF10 and NPPB than the cardiac tissue progenitors **(Fig. 5G,top; S7E,left)**. Multilineage progenitors also expressed higher levels of cardiac-enriched factors than the gut progenitors, such as the growth factors IGF1 and ANGPT1, and the ECM proteins DCN and LUM **(Fig. 5G,bottom; S7E,right)**. IGF1 enhances mesodermal cell differentiation and subsequent cardiac progenitor cell formation (*29*), and ANGPT1 supports proper atrium chamber morphogenesis (*29, 30*). DCN and LUM, matrix molecule genes enriched in the multilineage progenitors, contribute to the structure and mechanics of the heart by binding to core matrix proteins like collagen I and III, and facilitate thickening of collagen fibrils, respectively, thereby impacting collagen fibrillogenesis (*31, 32*). Hence, multilineage progenitors expressed increased levels of secreted factor genes relevant to both cardiac and gut tissue morphogenesis more than either individual tissue alone.

In summary, this analysis revealed that, in addition to the emergence of cardiac cells within the multilineage organoids, the co-development of intestine alongside cardiac cells potentially contributes to more structurally and functionally mature cardiac tissue via the secretion of key cardio-inductive molecules.

Discussion

Although organoids can recapitulate many physiologically-relevant properties of tissue development *in vitro*, they typically lack the cooperative paracrine interactions between adjacent tissues that characterize embryogenesis, as well as the multilineage progenitors essential for the development of complex organs such as the heart. Heart development relies on the complex contribution of progenitors derived from distinct germ lineages (mesoderm, ectoderm) and diverse paracrine factors (endoderm). Our attempts to generate cardiac organoids from mainly

cardiac-specified mesoderm spheroids resulted in poor growth, low cellular complexity, and limited functional maturation and diversity of cardiomyocytes (*14*). Here, we demonstrate a multi-tissue organoid model system capable of simultaneously producing both cardiac (mesoderm) and gut (endoderm) tissues in a sequentially emergent manner. This multilineage organoid recapitulates key structural and functional properties of the developing human heart, and suggests that gut-forming endoderm (i.e. MHG) contributes to atrial/nodal cardiac specification and maturation.

Aggregation of early committed mesendoderm progenitors derived from human iPSCs in permissive media conditions promoted the co-emergence of functional cardiac and gut-like tissues in a temporal sequence that mimics human embryonic morphogenesis. The co-emergence of cardiac and gut tissue paralleled organogenesis in the human embryo, in which initiation of the heart beat (3 weeks of gestation) is followed one week later by the extension of the gut tube into fore-, mid- and hind-gut structures (*33, 34*). At early stages of *in vitro* culture, multilineage organoids resemble human fetal heart formation (~5 weeks of gestation), evidenced by the formation of a surface layer of epicardial cells and a core of cardiomyocytes that exhibit significant growth over long-term culture. The epicardium is an important source of IGF2, a potent cardiac mitogen involved in cardiac wall thickening (*35, 36*), as well as cardiac fibroblasts and SMCs that invade the heart following an epithelial-to-mesenchymal transition (*37*). Similarly, in our organoid model, we observed cardiac expansion and WT1-positive cells outside the epicardial layer, as well as the later emergence of SMCs and endothelial cells (which occur at ~10 weeks of gestation in human fetal heart). The co-emergence of multiple key progenitor cells contributed to the cellular and structural complexity of the cardiac compartment of the multilineage organoids.

The presence of gut tissue developing alongside the cardiac tissue improved the phenotypic and functional maturation of the organoid cardiomyocytes. Additionally, whereas conventional microtissues (devoid of gut tissue) were primarily comprised of less mature, ventricular cardiomyocytes, cardiac/gut co-emergence promoted cardiomyocyte subtype specification into atrial/nodal-like cells. The current conventional view of atrial and ventricular cardiomyocytes specification is that the different cardiomyocyte subtypes derive from distinct mesoderm populations (*38, 39*). However, our organoid model demonstrated the emergence of predominantly cardiomyocytes with an atrial/nodal phenotype in parallel with primitive gut formation. Whereas at day 20, multilineage organoids contained equivalent amounts of ventricular (MLC2V+) and atrial/nodal cardiomyocytes (MLC2V-), by day 30 when primitive MHG structures emerged, the cardiac tissue had a higher proportion of atrial/nodal cardiomyocytes **(Fig. 2 D,E)**. Therefore, we speculate that MHG endoderm, similar to other endoderm subtypes, secretes factors that impact the development of the heart, and specifically promotes atrial/nodal specification. Indeed, previous studies showed that other endoderm derivatives, such as anterior visceral endoderm and anterior foregut, promote cardiac mesoderm specification and formation of new cardiomyocytes through the secretion of cardiac-inductive factors, like Activin A and FGF2 (*7, 40, 41*). FGF2 is also expressed by the epithelial, stromal, and SMCs in the intestine, however the functional effects on gut development have not been fully defined (*42, 43*). Our multilineage organoid model of cardiac and gut co-emergence offers a novel platform to investigate how neighboring tissues synergistically interact to promote co-development and maturation.

In the multilineage organoid model, cardiac tissue developed in parallel with intestinal tissue, whose cellular complexity mimics the small intestinal mucosa adjacent to enteric SMCs.

The formation of an enteric SMC layer in close proximity to the gut epithelium is notable since enteric SMCs have only previously been observed in gut organoids after *in vivo* transplantation (*44*). Furthermore, the SMCs in multilineage organoids exhibited spontaneous peristaltic-like contractility, which has only been observed in fully mature cells *in vivo*, or in *in vitro* cultures of primary cells together with stromal cells and gut pacemaker cells (interstitial cells of Cajal) seeded onto a scaffold (*45, 46*). In addition, other gut organoid models only achieve an intestine-like mucosa formation upon embedding in an exogenous extracellular matrix (i.e. Matrigel) (*44, 47*). Thus, our organoid model creates a microenvironment permissive for gut tissue formation in the absence of exogenous extracellular matrix components or morphogenic signaling cues, likely due, in part, to the enrichment in ECM components, such as glycosaminoglycans and hyaluronic acid, that facilitate embryonic morphogenesis.

Despite the robust emergence of the multilineage organoid phenotype in all spheroids within a single experiment, the reproducibility between experiments appeared to be dependent on subtle transcriptomic differences in the starting progenitor population. In addition to the multilineage organoids, gut organoids and cardiac microtissues formed with relatively equal frequencies originating from the same initial induction, tissue formation, and culture conditions. Gene expression analysis of the starting populations that gave rise to the different phenotypic outcomes indicated that multilineage organoids result from progenitors with enriched expression of several heart-related TFs, cardiomyocyte contractile machinery related genes, and SOX17, a definitive endoderm master regulator gene. The expression of endoderm-specific genes at the progenitor stage suggests that not all cells undergo the intended cardiac mesoderm commitment, and the subsequent emergence of intestine tissue in the multilineage organoids results from the permissive culture medium supporting the expansion and differentiation of the endoderm progenitors. The analysis of genes encoding secreted molecules in the gut organoid progenitors revealed high expression of FGF10, which functions as an autocrine and paracrine signaling molecule in heart development as well as in the intestine, by regulating the balance between goblet and paneth cells (*24, 25, 27*). Our multilineage organoid model will be useful for future studies dissecting paracrine interactions between cardiac and gut tissues, and identification of specific factors that promote morphogenesis and maturation of adjacent tissues.

Overall, our model represents a new class of organoids that encompasses the co-development and maturation of two distinct tissues arising from a mixed pool of mesendoderm progenitors. This organoid model opens new avenues to study genetic diseases that affect both the heart and the gut that have been challenging to investigate, such as chronical atrial and intestinal dysrhythmias (*48*). Organoids have been primarily developed with the intent to model individual tissues with higher order structural organization and physiologic function in isolation (*11, 44, 49*), and only limited attempts have been made to generate more complex and heterotypic organoids via fusion of pre-differentiated cells and/or organoid tissues (*50, 51*). In contrast, multilineage organoids demonstrate that distinct tissues can arise together in parallel within a single spheroid to synergistically support each other's development, and thus will be useful to advance the understanding of co-operative interactions during tissue co-development from early specification to structurally and functionally mature tissues (*52*). In a broader context, multilineage organoids represent a next step in the evolution of modeling developmental organogenesis *in vitro* and address complex multi-organ diseases.

References and Notes:

1. M. A. Lancaster, J. A. Knoblich, Organogenesis in a dish: Modeling development and disease using organoid technologies. *Science* **345**, (2014).
2. A. C. S. Oriane B. Matthys, Todd C. McDevitt, Engineering Human Organoid Development Ex Vivo - Challenges and Opportunities. *Current Opinion in Biomedical Engineering*, (2020).
3. H. T. Zhang, T. Hiiragi, Symmetry Breaking in the Mammalian Embryo. *Annual review of cell and developmental biology* **34**, 405-426 (2018).
4. J. Jung, M. Zheng, M. Goldfarb, K. S. Zaret, Initiation of mammalian liver development from endoderm by fibroblast growth factors. *Science* **284**, 1998-2003 (1999).
5. Y. Ishii, J. D. Langberg, R. Hurtado, S. Lee, T. Mikawa, Induction of proepicardial marker gene expression by the liver bud. *Development* **134**, 3627-3637 (2007).
6. D. Srivastava, Making or breaking the heart: from lineage determination to morphogenesis. *Cell* **126**, 1037-1048 (2006).
7. J. Lough, Y. Sugi, Endoderm and heart development. *Developmental dynamics : an official publication of the American Association of Anatomists* **217**, 327-342 (2000).
8. X. Lian *et al.*, Robust cardiomyocyte differentiation from human pluripotent stem cells via temporal modulation of canonical Wnt signaling. *Proc Natl Acad Sci U S A* **109**, E1848-1857 (2012).
9. X. Bao *et al.*, Long-term self-renewing human epicardial cells generated from pluripotent stem cells under defined xeno-free conditions. *Nat Biomed Eng* **1**, (2016).
10. X. Lian *et al.*, Directed cardiomyocyte differentiation from human pluripotent stem cells by modulating Wnt/beta-catenin signaling under fully defined conditions. *Nat Protoc* **8**, 162-175 (2013).
11. M. Takasato *et al.*, Kidney organoids from human iPS cells contain multiple lineages and model human nephrogenesis. *Nature* **536**, 238 (2016).
12. F. M. Gribble, F. Reimann, Enteroendocrine Cells: Chemosensors in the Intestinal Epithelium. *Annual review of physiology* **78**, 277-299 (2016).
13. X. Yang, L. Pabon, C. E. Murry, Engineering Adolescence: Maturation of Human Pluripotent Stem Cell-derived Cardiomyocytes. *Circulation research* **114**, 511-523 (2014).
14. H. K. Voges *et al.*, Development of a human cardiac organoid injury model reveals innate regenerative potential. *Development* **144**, 1118-1127 (2017).
15. E. Giacomelli *et al.*, Three-dimensional cardiac microtissues composed of cardiomyocytes and endothelial cells co-differentiated from human pluripotent stem cells. *Development* **144**, 1008-1017 (2017).
16. S. D. Lundy, W. Z. Zhu, M. Regnier, M. A. Laflamme, Structural and functional maturation of cardiomyocytes derived from human pluripotent stem cells. *Stem Cells Dev* **22**, 1991-2002 (2013).
17. H. D. Kim *et al.*, Human fetal heart development after mid-term: morphometry and ultrastructural study. *J Mol Cell Cardiol* **24**, 949-965 (1992).
18. A. W. Racca *et al.*, Contractile properties of developing human fetal cardiac muscle. *The Journal of physiology* **594**, 437-452 (2016).
19. N. Cao *et al.*, Ascorbic acid enhances the cardiac differentiation of induced pluripotent stem cells through promoting the proliferation of cardiac progenitor cells. *Cell Res* **22**, 219-236 (2012).

20. M. Wheelwright *et al.*, Investigation of human iPSC-derived cardiac myocyte functional maturation by single cell traction force microscopy. *PLoS ONE* **13**, e0194909 (2018).
21. V. Volpato, C. Webber, Addressing variability in iPSC-derived models of human disease: guidelines to promote reproducibility. *Dis Model Mech* **13**, (2020).
22. K. Brown *et al.*, eXtraembryonic ENdoderm (XEN) stem cells produce factors that activate heart formation. *PLoS ONE* **5**, e13446 (2010).
23. A. Holtzinger, G. E. Rosenfeld, T. Evans, Gata4 directs development of cardiac-inducing endoderm from ES cells. *Dev Biol* **337**, 63-73 (2010).
24. D. Al Alam *et al.*, Fibroblast growth factor 10 alters the balance between goblet and Paneth cells in the adult mouse small intestine. *Am J Physiol-Gastr L* **308**, G678-G690 (2015).
25. F. Rochais *et al.*, FGF10 promotes regional foetal cardiomyocyte proliferation and adult cardiomyocyte cell-cycle re-entry. *Cardiovasc Res* **104**, 432-442 (2014).
26. S. S. Chan *et al.*, Fibroblast growth factor-10 promotes cardiomyocyte differentiation from embryonic and induced pluripotent stem cells. *PLoS ONE* **5**, e14414 (2010).
27. R. G. Kelly, N. A. Brown, M. E. Buckingham, The arterial pole of the mouse heart forms from Fgf10-expressing cells in pharyngeal mesoderm. *Dev Cell* **1**, 435-440 (2001).
28. I. A. Sergeeva, V. M. Christoffels, Regulation of expression of atrial and brain natriuretic peptide, biomarkers for heart development and disease. *Biochim Biophys Acta* **1832**, 2403-2413 (2013).
29. M. C. Engels *et al.*, IGF promotes cardiac lineage induction by selective expansion of cardiogenic mesoderm in vitro. *European Heart Journal* **34**, 929-929 (2013).
30. K. H. Kim, Y. Nakaoka, H. G. Augustin, G. Y. Koh, Myocardial Angiopoietin-1 Controls Atrial Chamber Morphogenesis by Spatiotemporal Degradation of Cardiac Jelly. *Cell Rep* **23**, 2455-2466 (2018).
31. S. Chakravarti, Functions of lumican and fibromodulin: lessons from knockout mice. *Glycoconj J* **19**, 287-293 (2002).
32. Z. Ferdous, V. M. Wei, R. Iozzo, M. Höök, K. J. Grande-Allen, Decorin-transforming growth factor- interaction regulates matrix organization and mechanical characteristics of three-dimensional collagen matrices. *The Journal of biological chemistry* **282**, 35887-35898 (2007).
33. M. A. Hill, Embryology Gastrointestinal Tract Development (2020).
34. M. A. Hill, Embryology Cardiovascular System - Heart Development (2020).
35. H. Shen *et al.*, Extracardiac control of embryonic cardiomyocyte proliferation and ventricular wall expansion. *Cardiovasc Res* **105**, 271-278 (2015).
36. J. M. Perez-Pomares, J. L. de la Pompa, Signaling during epicardium and coronary vessel development. *Circ Res* **109**, 1429-1442 (2011).
37. A. M. Smits, E. Dronkers, M. J. Goumans, The epicardium as a source of multipotent adult cardiac progenitor cells: Their origin, role and fate. *Pharmacol Res* **127**, 129-140 (2018).
38. J. H. Lee, S. I. Protze, Z. Laksman, P. H. Backx, G. M. Keller, Human Pluripotent Stem Cell-Derived Atrial and Ventricular Cardiomyocytes Develop from Distinct Mesoderm Populations. *Cell Stem Cell* **21**, 179-194 e174 (2017).
39. W. P. Devine, J. D. Wythe, M. George, K. Koshiba-Takeuchi, B. G. Bruneau, Early patterning and specification of cardiac progenitors in gastrulating mesoderm. *Elife* **3**, (2014).

40. Y. Sugi, J. Lough, Activin-A and FGF-2 mimic the inductive effects of anterior endoderm on terminal cardiac myogenesis in vitro. *Dev Biol* **168**, 567-574 (1995).
41. C. Mummery *et al.*, Differentiation of human embryonic stem cells to cardiomyocytes: role of coculture with visceral endoderm-like cells. *Circulation* **107**, 2733-2740 (2003).
42. A. U. Dignass, A. Sturm, Peptide growth factors in the intestine. *Eur J Gastroenterol Hepatol* **13**, 763-770 (2001).
43. I. el-Hariry, M. Pignatelli, N. Lemoine, Fibroblast growth factor 1 and fibroblast growth factor 2 immunoreactivity in gastrointestinal tumours. *J Pathol* **181**, 39-45 (1997).
44. J. O. Munera *et al.*, Differentiation of Human Pluripotent Stem Cells into Colonic Organoids via Transient Activation of BMP Signaling. *Cell Stem Cell* **21**, 51-64 e56 (2017).
45. D. Gays *et al.*, An exclusive cellular and molecular network governs intestinal smooth muscle cell differentiation in vertebrates. *Development* **144**, 464-478 (2017).
46. M. Kobayashi *et al.*, Bioengineering functional smooth muscle with spontaneous rhythmic contraction in vitro. *Sci Rep* **8**, 13544 (2018).
47. T. Sato *et al.*, Single Lgr5 stem cells build crypt-villus structures in vitro without a mesenchymal niche. *Nature* **459**, 262-U147 (2009).
48. P. Chetaille *et al.*, Mutations in SGOL1 cause a novel cohesinopathy affecting heart and gut rhythm. *Nat Genet* **46**, 1245-1249 (2014).
49. M. Takasato *et al.*, Kidney organoids from human iPS cells contain multiple lineages and model human nephrogenesis. *Nature* **526**, 564-568 (2015).
50. H. Koike *et al.*, Modelling human hepato-biliary-pancreatic organogenesis from the foregut-midgut boundary. *Nature* **574**, 112-116 (2019).
51. Y. Xiang *et al.*, Fusion of Regionally Specified hPSC-Derived Organoids Models Human Brain Development and Interneuron Migration. *Cell Stem Cell* **21**, 383-398 e387 (2017).
52. J. M. Faustino Martins *et al.*, Self-Organizing 3D Human Trunk Neuromuscular Organoids. *Cell Stem Cell* **26**, 172-186 e176 (2020).
53. N. Huebsch *et al.*, Automated Video-Based Analysis of Contractility and Calcium Flux in Human-Induced Pluripotent Stem Cell-Derived Cardiomyocytes Cultured over Different Spatial Scales. *Tissue Eng Part C Methods* **21**, 467-479 (2015).
54. M. A. Mandegar *et al.*, CRISPR Interference Efficiently Induces Specific and Reversible Gene Silencing in Human iPSCs. *Cell Stem Cell* **18**, 541-553 (2016).
55. T. A. Hookway, J. C. Butts, E. Lee, H. Tang, T. C. McDevitt, Aggregate formation and suspension culture of human pluripotent stem cells and differentiated progeny. *Methods (San Diego, Calif.)* **101**, 11-20 (2016).
56. D. Turaga *et al.*, Single cell determination of cardiac microtissue structure and function using light sheet microscopy. *Tissue Eng Part C Methods*, (2020).
57. D. C. Nguyen *et al.*, Microscale generation of cardiospheres promotes robust enrichment of cardiomyocytes derived from human pluripotent stem cells. *Stem Cell Reports* **3**, 260-268 (2014).
58. D. Kim, J. M. Paggi, C. Park, C. Bennett, S. L. Salzberg, Graph-based genome alignment and genotyping with HISAT2 and HISAT-genotype. *Nature biotechnology* **37**, 907-915 (2019).
59. Y. Liao, G. K. Smyth, W. Shi, featureCounts: an efficient general purpose program for assigning sequence reads to genomic features. *Bioinformatics (Oxford, England)* **30**, 923-930 (2014).

60. J. Feng *et al.*, GFOLD: a generalized fold change for ranking differentially expressed genes from RNA-seq data. *Bioinformatics (Oxford, England)* **28**, 2782-2788 (2012).
61. Z. Zhang *et al.*, Novel Data Transformations for RNA-seq Differential Expression Analysis. *Scientific reports* **9**, 4820 (2019).

Acknowledgments:

The authors would like to thank the Stem Cell Core (Dr. Po-Lin So), Histology and Light Microscopy Core (Dr. Meredith Calvert) and Genomics Core (Dr. Natasha Carli and Jim McGuire) at the Gladstone Institutes, and Electron Microscopy Lab (Dr. Danielle Jorgens) at UC Berkeley for all the help and expertise shared. The authors thank Dr. Bruce Conklin laboratory for providing WTC11 GCaMP iPS cell line, Dr. Deepak Srivastava's laboratory for providing antibodies against MYL2 and MYL3, and Dr. Katja Schenke-Layland for providing human fetal heart paraffin blocks. A special thanks to Drs. Tracy Hookway, Irfan Kathiriya, Sanjeev Ranade and Elphège Nora for relevant critical discussion. The authors also acknowledge the Gladstone Scientific Editing Department (Drs. Francoise Chanut and Kathryn Claiborn) for assistance with manuscript editing. This work was supported by the California Institute of Regenerative Medicine Grant S02708 and the Gladstone BioFulcrum Heart Failure Research Program. **Author contributions:** A.C.S. and T.C.M. conceived the study, interpreted the data, and wrote the manuscript. A.C.S. performed iPSC differentiations, microtissues formation and maintenance, histology studies, preparation of the cells for patch clamp analysis, calcium imaging, bulk and single-cell RNA-seq experiments and scRNA-seq analysis. O.B.M. acquired and analyzed calcium flux analysis, assisted on microtissues maintenance. M.H.L. performed patch clamp data acquisition and analysis. D.A.J. developed the python script for calcium flux and patch clamp analysis, performed the alignment of single-cell and bulk RNA-seq data and assisted with the single-cell and bulk RNA-seq analysis. M.A.K. and V.N. prepared bulk RNA-seq libraries and assisted in microtissue maintenance. D.T. performed light sheet microscopy and analysis. M.A. and B.G.B. assisted with bulk RNA-seq data analysis and B.G.B. contributed to experimental design and interpretation of results. O.B.M., D.A.J., M.A.K, V.N., M.A., and B.G.B. contributed to manuscript editing and discussion. **Competing interests:** T.C.M. is a consultant for Tenaya Therapeutics. B.G.B. is a co-founder of and owns equity in Tenaya Therapeutics. The other authors declare no competing interests. **Data and material availability:** Raw data is available at Geo under the accession number [upload in progress].

Supplementary Materials:

Materials and Methods

Figures S1-S7

Tables S1

Movies S1-S8

References (*8-9; 53-61*)

Figures:

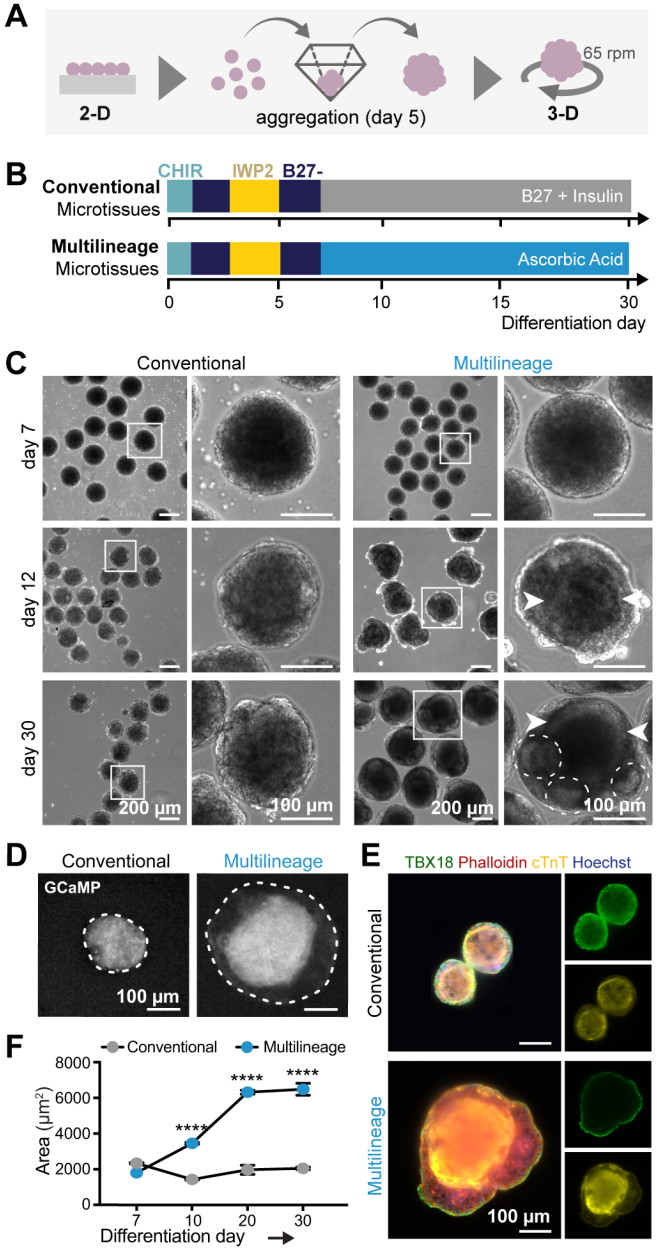

Fig. 1. Derivation of a multilineage organoid with complex cardiac structures. **A-B** Overall schematic of conventional and multilineage microtissue formation. **C.** Brightfield images of conventional and multilineage microtissues over the course of 30 days in cell culture; high magnification views of the regions within white squares (right). Multilineage microtissues develop a compact dark core of cells (arrowheads) and epithelial-like structures (dashed line) at the surrounding translucent region. **D.** Calcium flux transients (GCAMP+) were limited to the center area of the multilineage microtissues in comparison with conventional microtissues. Dashed line, microtissue boundaries. **E.** Representative light-sheet imaging of microtissues stained for cardiac Troponin T (cTnT) and TBX18. Conventional microtissues are composed of cardiomyocytes positive for cTnT and TBX18, whereas multilineage microtissues contain a core

of cardiomyocytes (cTnT+/TBX18-) surrounded by stromal-like cells positive for phalloidin and an outer layer of epicardial-like cells (TBX18+), mimicking an in vivo heart wall. Dashed line, epithelial-like structures. **F.** Multilineage microtissues display an increase in surface area throughout culture. Representative experiment. Conventional vs. Multilineage, ****$p<0.0001$.

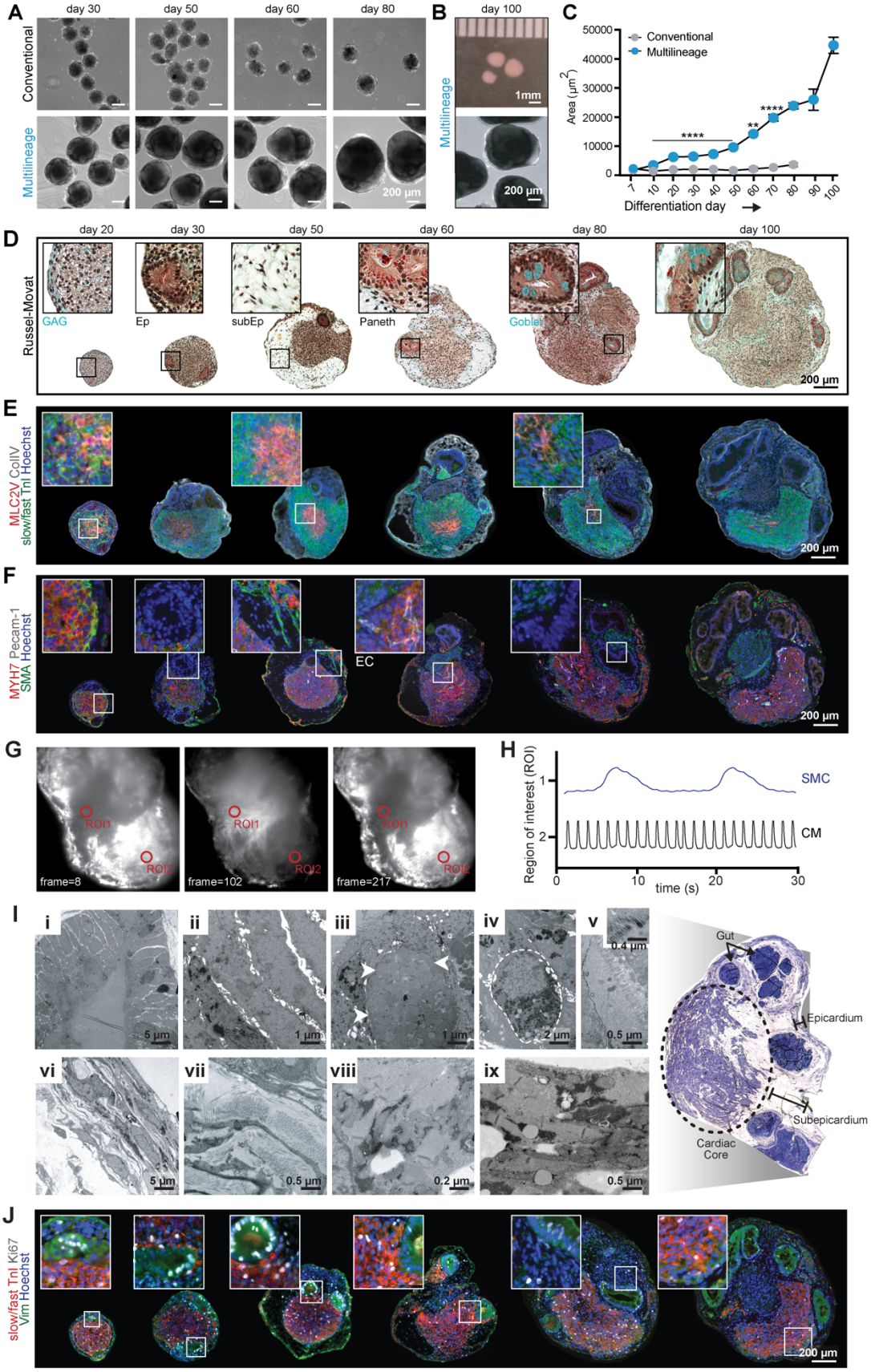

Fig. 2. Long-term culture of multilineage organoids recapitulates early heart and gut development. **A.** Brightfield microscopy images of conventional and multilineage tissue growth from days 30-80 of culture. Conventional microtissues viable until day 80. **B.** Day 100 multilineage organoid brightfield (bottom) and stereoscope macroscopy (top) images. **C.** Multilineage organoids display an increase in surface area until day 100 of culture. Representative experiment. Conventional vs. Multilineage, **p<0.005, ****p<0.0001. **D-F.** Structural dynamics and cell composition of multilineage organoids over the course of the culture depicted by Russel-Movat stain (D) and fluorescent immunostaining (E-F). **G-H.** Representative images (G) and traces (H) of spontaneous calcium flux transients of the smooth muscle cells (SMC) (ROI 1) and cardiomyocytes (CM) (ROI 2) of a multilineage organoid imaged via light sheet microscopy (Movie S6). **I.** Transmission electron microscopy of the gut structures (i-v), epicardium/subepicardium (vi-vii) and cardiac core (viii-ix). GAG, glycosaminoglycans; Ep, epithelial-like structures; subEp, subepicardium-like tissue; Endo, endothelial cells network; Arrowheads, goblet cell (iii); Dashed line, paneth cell (iv). **J.** Multilineage organoid demonstrated a decreased in cell cycle active cells (Ki67+) over time.

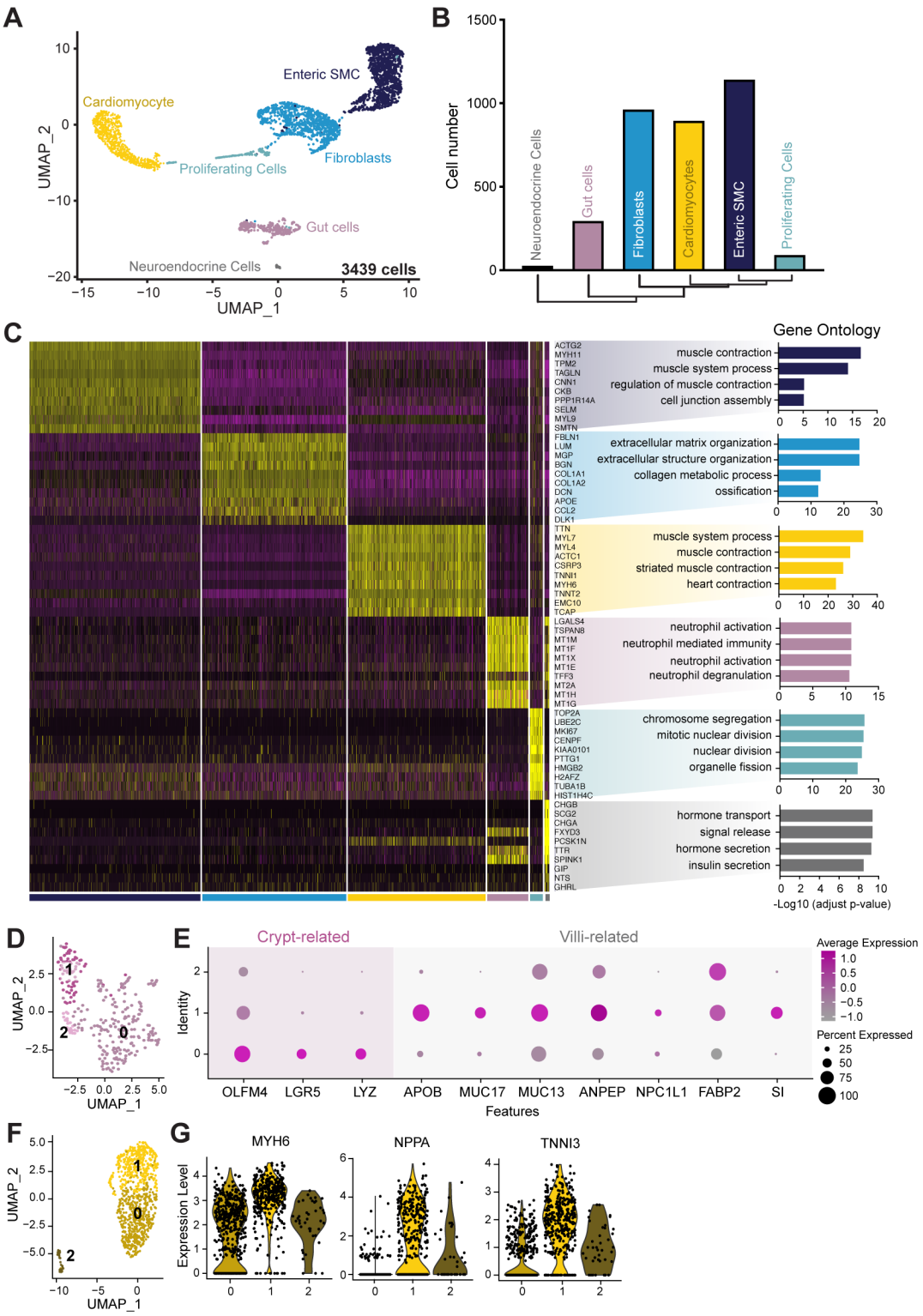

Fig. 3. Single cell RNA-sequencing at day 100 reveals complex cellular heterogeneity of multilineage organoids. **A.** UMAP plot of all cellular populations identified. **B.** Cell populations grouped according to similarity (x axis) and cell number (y axis). **C.** Heatmap of top 10 differential expressed genes that defines each cell cluster and associated biological processes gene ontology analysis. **D-E.** A sub-clustering analysis of the gut cells evidenced 3 main cell

clusters (D): cluster 0 composed mainly by crypt cells (OLFM4, E), such as gut stem cells (LGR5; E) and paneth cells (LYZ; E); and cluster 1 and 2, constituted by cells at the villi, the enterocytes, identified by the expression of genes related to transmembrane mucins (MUC13, MUC17; E), digestion (ANPEP, FABP2, SI; E) and cholesterol transporter genes (NPC1L1; E), as well as APOB (E), a gene expressed in the small intestine. **F-G.** A subset analysis of the cardiomyocyte cluster highlight (F) 3 main clusters of cardiomyocytes: cluster 0 and 2 composed of more immature cardiomyocytes; and cluster 1, comprised of more transcriptomically mature atrial/nodal cells (cluster 1; G) through high number of cells expressing MYH6, NPPA and TNNI3 (G).

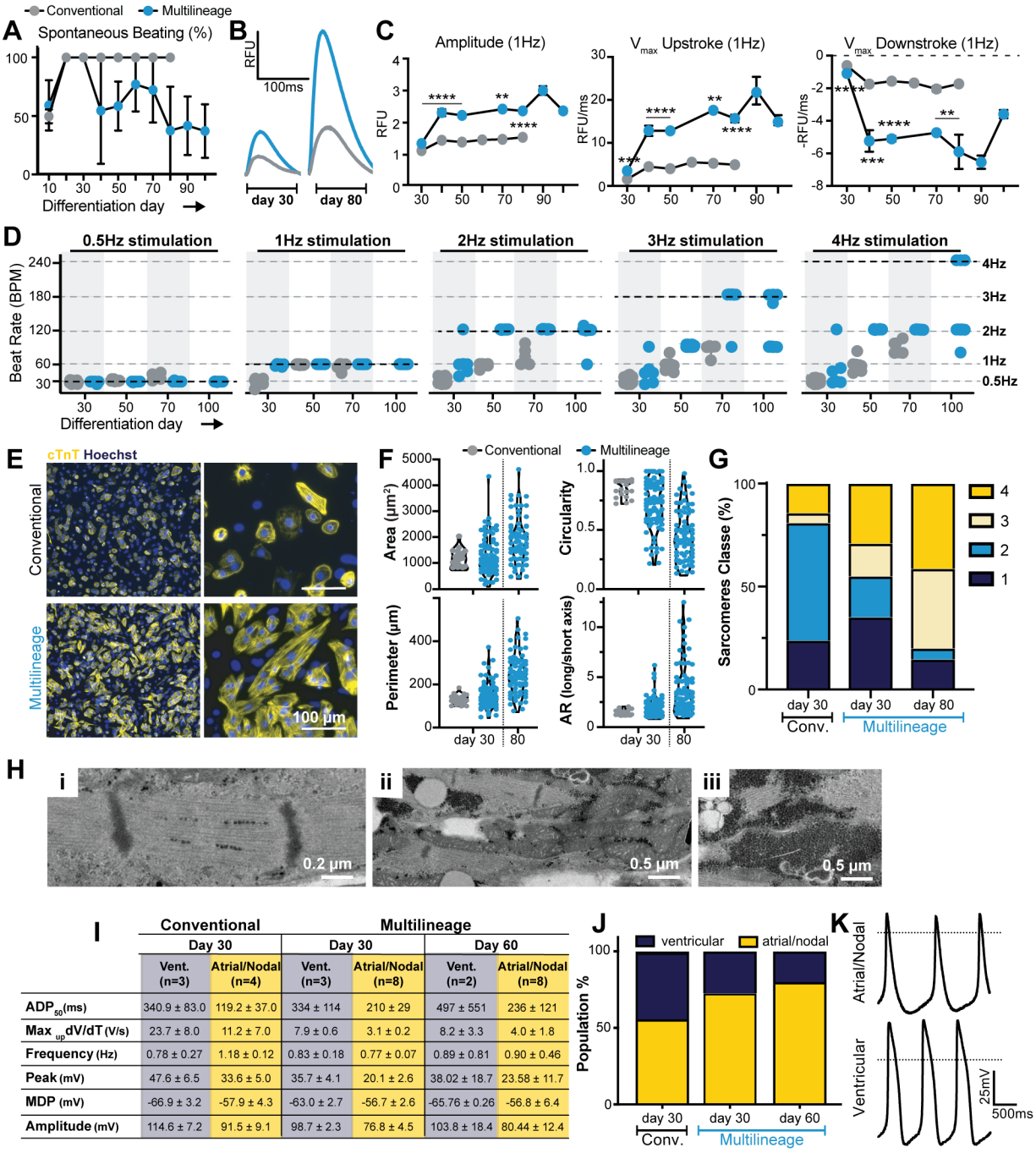

Fig. 4. Cardiomyocytes from multilineage organoids display phenotypic and functional maturation throughout culture, and preferentially specify into atrial/nodal-like cells. **A.** Multilineage organoids demonstrated a reduction in spontaneous beating throughout culture. **B.** Representative calcium flux traces at day 30 and 80 of culture. **C.** Cardiomyocytes at multilineage organoids display mature calcium flux features by showing higher amplitude, Vmax upstroke and downstroke. Conventional vs. Multilineage, **p<0.01, **p<0.005, ***p<0.001, ****p<0.0001. **D.** Cardiomyocytes able to respond to electrical stimuli throughout culture. **E.** Representative immunofluorescence images of dissociated cardiomyocytes from conventional

microtissues and multilineage organoids. **F.** Cardiomyocyte structural feature metrics. **G.** Cardiomyocyte sarcomere classification (class1- not defined sarcomeres, more immature; class 4- parallel organized, striped pattern sarcomeres, more mature). **H.** Day 100 multilineage organoid cardiomyocyte sarcomeres (i), intercalated disks (ii, arrow heads) and glycogen reservoir ultrastructure (iii). **I.** Table with detailed information regarding cardiomyocyte subtype electrophysiology metrics. **J.** Percentage of ventricular and atrial/nodal cardiomyocytes dissociated from conventional microtissues and multilineage organoids. **K.** Representative traces of ventricular and atrial/nodal cardiomyocytes in multilineage organoids at day 30 of culture.

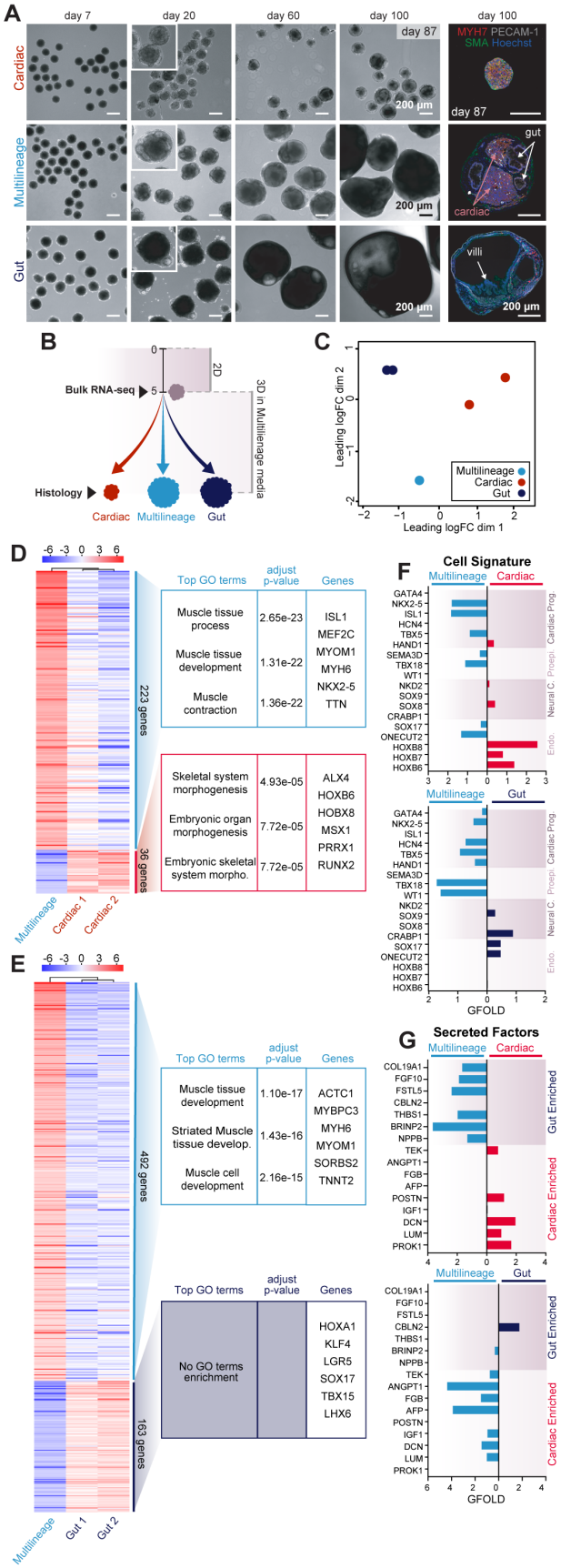

Figure 5. Multilineage organoid progenitor cells have a transcriptomic profile that supports the co-development of cardiac and gut tissues. **A.** Histological analysis spheroid phenotypic diversity between experiments. **B.** Experimental work flow schematic. **C.** Multidimensional scaling (MDS) plot describes similarity between the progenitor cells that give rise to cardiac microtissues and multilineage and gut organoids. **D.** Heat map of the pairwise comparison of multilineage organoids and cardiac microtissue progenitors and respective gene ontology (GO) terms and genes evidenced a gene transcription profile that favors heart tissue formation. **E.** Heat map of the pairwise comparison of multilineage organoid and gut organoid progenitors and respective GO terms and genes demonstrated that multilineage progenitor gene expression supports cardiac tissue formation. **F-G.** Targeted pairwise comparison of cardiac vs. multilineage (top) and gut vs. multilineage (bottom) progenitor cells regarding: key cell signature genes for cardiac progenitors (Cardiac Prog.), proepicardium (Proepi.), neural crest (Neural C.) and endoderm-derived cells (Endo.) demonstrated that the multilineage organoid progenitors cells expressed key heart and endoderm related transcription factors (F); and that secreted factors highly expressed in gut organoid and cardiac microtissues progenitor cells were highly expressed in the multilineage organoid progenitors (G).